Carbohydrate Polymers 87 (2012) 2038–2045

Contents lists available at SciVerse ScienceDirect

Carbohydrate Polymers

journal homepage: www.elsevier.com/locate/carbpol

Superabsorbent hydrogel composite made of cellulose nanofibrils and chitosan-*graft*-poly(acrylic acid)

Cristiane Spagnol[a], Francisco H.A. Rodrigues[a,b], Antonio G.B. Pereira[a], André R. Fajardo[a,*], Adley F. Rubira[a], Edvani C. Muniz[a]

[a] Grupo de Materiais Poliméricos e Compósitos (GMPC) – Departamento de Química, Universidade Estadual de Maringá, Av. Colombo, 5790, 87020-900 Maringá, Paraná, Brazil
[b] Coordenação de Química, Universidade Estadual Vale do Acaraú, Avenida da Universidade, 850, Campus da Betânia, 62040-370 Sobral, Ceará, Brazil

ARTICLE INFO

Article history:
Received 19 August 2011
Received in revised form 6 October 2011
Accepted 7 October 2011
Available online 14 October 2011

Keywords:
Hydrogel composites
Cellulose nanofibrils
Superabsorbent hydrogels
Swelling properties
Chitosan

ABSTRACT

Superabsorbent hydrogel composites based on cellulose nanofibrils and chitosan-*graft*-poly(acrylic acid) copolymer were developed in this work. The FTIR data showed that the copolymerization and the composite formation reaction were successfully performed. In addition, the XRD pattern indicated that the nanofibrils crystallinity was as high as 90%. A 2^{4-1} fractional factorial design was employed to evaluate the effect of acrylic acid/chitosan molar ratio, crosslinker, initiator, and filler in the swelling capacity of hydrogel composites. By the analysis of variance (ANOVA), including *F*-test and *P*-values, it was found that the crosslinker and filler correspond to 40% and 30% of the evaluated response, respectively. The addition of nanofibrils provided faster equilibrium conditions as well as improved the swelling capacity in ca. 100 units, from 381 to 486. SEM images showed that the addition of nanofibrils into the hydrogel matrix increased the averaged-dimension of porous. Finally, the composites showed responsive behavior in relation to pH and salt solution. Such characteristics make these smart materials suitable for several technological applications.

1. Introduction

Cellulose, chitin, and chitosan contain in their structures amorphous regions susceptible to acid attack allowing the formation of nanofibrils (De Mesquita, Donnici, & Pereira, 2010; Muzzarelli, 2011; Zhou, Wu, Yue, & Zhang, 2011). These fibrils in nano scale (nanofibrils) show excellent dispersion in water, easy to obtain, to handle and to mold (Li, Zhou, & Zhang, 2009; Nakagaito, Fujimura, Sakai, Hama, & Yano, 2009). In addition, nanofibrils are able to form interactions among the nanosized moieties that form a percolated network connected by hydrogen bonds, providing good dispersion of them in the polymeric matrix (Azeredo et al., 2010; Liang, Zhang, Li, & Xu, 2007). These characteristics allow the application of nanofibrils as filler in several polymeric matrices as reinforcing agents (Peresin et al., 2010; Teixeira et al., 2009). Despite these advantages, the use of cellulose nanofibrils as fillers in hydrogels matrix is poorly explored. Therefore, the aims of this work is to develop superabsorbent hydrogels composite made of cellulose nanofibrils and chitosan-*graft*-poly(acrylic acid) and evaluate the potentialities of use of them.

Chitosan is a well-known polymer derived from the biopolymer chitin, shows interesting physical, chemical and biological properties (biocompatibility, biodegradability, low toxicity, antibacterial and hemostatic activities and chelating potential) (Ebringerová, Hromádková, & Heinze, 2005; Muzzarelli, 2009; Wang, Li, Luz, & Wang, 1997). Therefore, chitosan acts as a desirable backbone to graft poly(acrylic acid) forming a superabsorbent material (Paulino et al., 2009). Superabsorbent hydrogels (SH) are water insoluble and are able to absorb and retain large amounts of aqueous fluids even under pressure. Therefore, SH exhibit great advantages over traditional water-absorbent materials. As a result, SH have aroused huge interest and consequently, these materials have been applied in several fields, such as hygienic products, horticulture, drug delivery systems, as well as water blocking tapes, and coal dewatering (Bajpai & Giri, 2002; Hill, 2007; Li, Liu, & Wang, 2005; Omidian, Rocca, & Park, 2005). However, the use of chitosan to form superabsorbent materials has been limited because of their usually poor mechanical properties when compared to other polymers. The addition of reinforcing fillers into the hydrogel matrix can enhance their mechanical properties and improve their handling.

In this present work, a fractional factorial design (2^{4-1}) was performed for evaluating the influence of some factors on the swelling degree of the hydrogels composites. The study seems to be suitable for understanding how such factors are related to each other and to the swelling degree. Furthermore, the addition of cellulose

* Corresponding author. Tel.: +55 44 3011 3676; fax: +55 44 3011 3676.
E-mail address: drefajardo@hotmail.com (A.R. Fajardo).

0144-8617/$ – see front matter © 2011 Elsevier Ltd. All rights reserved.
doi:10.1016/j.carbpol.2011.10.017

Table 1
Design of experiments.

Sample	2 level factors				
	A – AA/CTS ratio (mol%)	**B** – Crosslinker (wt%)[a]	**C** – Initiator (wt%)[b]	**D** – Filler (wt%)[c]	Water uptake ($g_{water}/g_{absorbent}$)
1	(−1) 5	(−1) 1	(−1) 1	(−1) none	204 ± 4
2	(+1) 10	(−1) 1	(−1) 1	(+1) 10	486 ± 7
3	(−1) 5	(+1) 3	(−1) 1	(+1) 10	249 ± 5
4	(+1) 10	(+1) 3	(−1) 1	(−1) none	127 ± 3
5	(−1) 5	(−1) 1	(+1) 3	(+1) 10	207 ± 5
6	(+1) 10	(−1) 1	(+1) 3	(−1) none	361 ± 6
7	(−1) 5	(+1) 3	(+1) 3	(−1) none	72 ± 3
8	(+1) 10	(+1) 3	(+1) 3	(+1) 10	273 ± 5
9	(0) 7.5	(0) 2	(0) 2	(−1) none	264 ± 5
10	(0) 7.5	(0) 2	(0) 2	(+1) 10	372 ± 7

[a] % of MBA.
[b] % of KPS.
[c] % of cellulose nanofibrils.

nanofibrils into the chitosan-*graft*-poly(acrylic acid) SH matrix, the effect of salt and pH in the swelling degree were investigated.

2. Experimental

2.1. Materials

Acrylic acid (Sigma–Aldrich, USA), potassium persulfate (Sigma–Aldrich, USA) and *N*,*N*′-methylenebisacrylamide (Pharmacia Biotech, USA). Chitosan (from Golden-Shell Biochemical, China), 85% deacetylated, presenting viscometric molar mass (M_V) of 87,000 g mol^{-1}. The M_V was obtained from the average intrinsic viscosity according to methodology previously described by Fajardo, Piai, Rubira, and Muniz (2010). All reactants possess analytical grade and were used without further purification.

2.2. Cellulose nanofibrils

Cotton fibers were purchased from Cocamar, a local agribusiness cooperative (Maringá, Paraná, Brazil). The fibers were firstly washed in a NaOH solution (2 wt%), under mechanic stirring for 1 h at room temperature, to remove some impurities (waxy, for instance). After this, the fibers were soaked in deionized water for 1 h at 80 °C and then dried in oven for 5 h at 50 °C. The cellulose nanofibrils were obtained through acid hydrolysis reaction using concentrate HCl at 45 °C for 1 h under vigorous magnetic stirring at cellulose/HCl ratio equal to 1/20 (g/mL). After this step, the resulting solution was centrifuged at 10,000 rpm for 5 min and washed using deionized water up to pH 7. The resultant material was lyophilized (at −57 °C for 48 h). Then, nanofibrils were characterized by Fourier transformed infrared spectroscopy technique (FTIR), X-ray diffraction (XRD), and transmission electronic microscopy (TEM).

2.3. Preparation of chitosan-graft-poly(acrylic acid)/cellulose nanofibrils hydrogel composites

A set of hydrogel composites based on chitosan, acrylic acid, and cellulose nanofibrils was synthesized according to the following procedure: an appropriate amount of chitosan was solubilized under magnetic stirring in 30 mL of acetic acid solution (1 v/v%) in a three-neck flask equipped with a reflux condenser, a funnel, and a $N_{2(g)}$ line. The chitosan-solution was bubbled with $N_{2(g)}$ for 30 min to remove the oxygen. Afterward, the solution was heated to 70 °C, and then 0.10 g of potassium persulfate was added to generate free radicals on the functional groups from chitosan. After 10 min, a solution consisting of 3.60 g acrylic acid, specific amounts of *N*,*N*′-methylenebisacrylamide (crosslinking agent), cellulose nanofibrils (filler) and 5 mL of water were added. The temperature was maintained in 70 °C and the system was stirred for further 2 h. The resultant granular products were cooled to room temperature and then neutralized to pH 7.0 through the dropping of NaOH solution (1 mol L^{-1}). The obtained material was washed with large volumes of distilled water to remove residual reactants and then oven-dried at 70 °C. The sizes of particles fall within 9–24 mesh range (2.00–0.71 mm). In addition, a blank sample hydrogel, without cellulose nanofibrils, was prepared according to procedures described above. This sample was labeled as chitosan-*graft*-poly(acrylic acid).

2.4. Statistical parameters evaluation by a factorial design approach

The influence of some parameters on the water uptake capacity of the chitosan-*graft*-poly(acrylic acid)/cellulose nanofibrils hydrogel composite was investigated by a 2^{4-1} fractional factorial design (FFD) in which four variables were tested: **A** – acrylic acid/chitosan molar ratio (numeric variable); **B** – crosslinker (numeric variable); **C** – initiator (numeric variable); **D** – filler (categoric variable). Each variable was fixed in two levels and duplicated-central point was employed, resulting at all in 10 runs. The coded variables (−1), (0) and (+1) represent the low, intermediate and high levels (see Table 1). The FFD and the evaluation of results, based on analysis of variance (ANOVA), were carried out by the use of Design Expert® (version 7.1.3) software.

2.5. Methods of characterization

All the dried hydrogel composites and the blank sample were characterized by FTIR spectroscopy technique (Shimadzu Scientific Instruments, Model 8300), in an equipment operating in the region from 4000 to 500 cm^{-1}, resolution of 4 cm^{-1}. The dried material was blended with KBr powder and pressed into tablets before spectrum acquisition. The XRD patterns were obtained in a diffractometer (DMAXB, Model Rigaku) equipped with a Cu-K$_($ radiation source (30 kV and 20 mA) in scattering angle range (2$($) from 5° to 70°, with resolution of 0.02°, at a scanning speed of 2° min^{-1}.

The hydrogel composites morphologies were evaluated through SEM images obtained from scanning electron microscope (Shimadzu, Model SS550 Superscan). The samples were gold-coated by sputtering technique before analyses. TEM images of the as-obtained cellulose nanofibrils and chitosan-*graft*-poly(acrylic acid)/cellulose nanofibrils hydrogel composite were taken in a transmission electron microscopy TOPCON 002B. For the CNWs, a suspension containing the cellulose nanofibrils was deposited on the grid (carbon-Formvar-coated copper) and left to dry at room temperature. For the chitosan-*graft*-poly(acrylic acid)/cellulose nanofibrils, a small droplet containing the hydrogel composite

Table 2
ANOVA of swelling: effect of molar ratio (**A**), crosslinker (**B**) and filler (**D**).

Source	Sum of squares	DF	Mean square	*F*-Value	*P*-ValueProb > *F*
Model	1.24×10^5	4	3098.37	62.41	0.0032 *sig*[a]
A – Molar ratio	21,528.12	1	21,528.12	43.36	0.0071
B – Crosslinker	50,721.13	1	50,721.13	102.17	0.0021
D – Filler	37,950.12	1	37,950.12	76.44	0.0032
AB	8256.12	1	8256.12	16.63	0.0266
Residual	1489.38	3	496.46		
Cor total	1.31×10^5	9			

[a] Model significant (R^2 = 0.9881; Adj R^2 = 0.9723).

fraction was placed on the grid and the solvent was evaporated at room temperature. The images were taken at 200 kV acceleration voltage (point resolution 0.18 nm).

2.6. Study of swelling properties

2.6.1. Swelling assays

Initially, the swelling assays were employed for evaluating the water absorption capacity of such materials (chitosan-*graft*-poly(acrylic acid) and chitosan-*graft*-poly(acrylic acid)/cellulose nanofibrils). In this way, ca. 15 mg of each sample to be tested were placed in 30 mL filter crucibles (porosity no. 0) pre-moistened and with a dry outer wall. This set was placed in water in such a way that the gel was completely submerged.

The crucible/composite hydrogel samples sets were removed at various time intervals, with the external wall of the set dried and the system weighed. The experimental set was done in triplicate (n = 3). The swelling capacity of the hydrogel composites was determined from equation:

$$W = \left[\frac{m}{m_0}\right] - 1 \quad (1)$$

where W is the gained water mass (in grams) per gram of composite hydrogel (absorbent), m is the mass of the swollen absorbent and m_0 is the mass of the dry material (Zhang, Rakotondradany, Myles, Fenniri, & Webste, 2009). The size distribution of the hydrogel composites remained in the 9–24 mesh range.

2.6.2. Effect of salt solution on water absorption

The hydrogel composites were immersed in distinct salt aqueous solutions (concentration: 0.15 mol L^{-1}) and their swelling capabilities were determined according to the procedures described previously. Aqueous solutions of NaCl, $CaCl_2$, and $AlCl_3$, at 25.0 °C, were used as swelling fluid. All solutions presented constant ionic strength (I = 0.1 M).

2.6.3. Evaluation of pH effect on swelling capability of hydrogel composites

The effect of the pH on the swelling was also evaluated using buffer solutions (pHs 2–12). The ionic strength was kept constant, 0.1 M.

3. Results and discussion

3.1. The evaluation through 2^{4-1} fractional factorial design (FFD)

Table 1 presents the used levels of all factors and the respective response (the water uptake capacity) for each run.

The main and the interaction effects were evaluated from the 10 experiments made to complete the FFD by the analysis of variance (ANOVA). The ANOVA is a statistical method in which allow evaluating how different sources of variation contributes to the observed variance for a particular variable (Zheng, Liu, & Wang, 2011). The ANOVA showed that the main effects **A**, **B**, **D**, and the interaction effect **AB** (see Table 1) are significant, since those effects presented *P*-values (*F*-test) smaller than 0.05, which means that the probability of the null hypothesis to be true is lesser than 5%. In other words, the observed changes on the response are not due to the random errors associated to the measures but rather to the changes in the level of **A**, **B** and **D** inputs, indeed.

Table 2 presents the data of ANOVA obtained through 2^{4-1} factorial design. The mathematic model, in terms of coded factors, which gives the swelling value (S) as function of significant effects is represented by equation

$$S = 259.88 + 51.87\mathbf{A} - 79.63\mathbf{B} + 68.87\mathbf{D} - 32.12\mathbf{AB} \quad (2)$$

The *F*-value for the model (Eq. (2)) is 62.41 and this implies that such model is statistically significant. There is only 0.32% of confidence that this "model *F*-value" could occur due to noise. The residual values explain the differences between predict values (model) and the observed ones (experimental). The data is distributed normally if all the points fall close to the straight line in the normal plot of residual. From Fig. 1a, which is referent to the normal plot of residuals, is quite evident that the residues falling in the range from +1.44 to −1.44 follow a normal distribution which strengths the *F*-test. According to the R^2 value (ca. 0.988), it is possible to infer that the model fits very well the experimental data.

The data are distributed normally or not from the graphical representation of the normal probability plot according to the statistical evaluation. From Fig. 1b, which is referent to the normal plot of effects, the disregarded values are normally distributed with mean equal zero and the points follow the straight line in the graph, while the significant effects do not follow the line. Fig. 1c and d shows the response surfaces obtained from the 2^{4-1} factorial design. The individual contribution of each variable to the evaluated response was 16.41% to **A** – molar ratio (acrylic acid/chitosan), 38.66% to **B** – crosslinker, 28.93% to **D** – filler, and 6.29% to **AB** interaction. The most influencing variable is the crosslinker, with almost 40% of contribution in the response, followed by the filler (nanofibrils), with ca. 30% of contribution.

3.2. Characterization

The FTIR spectra of raw cotton fibers and cellulose nanofibrils are quite similar. They presented bands at 3344, 2900, and 1646 cm^{-1}, which are assigned to stretching of –OH groups, C–H stretching, and –OH bending of the adsorbed water. Therefore, the bands of H–C–H and O–C–H in-plane bending vibrations appeared at 1432 cm^{-1} and the C–H deformation vibration appeared at 1367 cm^{-1}. The C–O–C, C–C–O, and C–C–H deformation modes and stretching vibrations, in which the motions of the C-5 and C-6 atoms were observed at 898 cm^{-1}, and the band referent to the C–OH out-of-plane bending at 670 cm^{-1} (Oh, Yoo, Shin, & Seo, 2005; Satyamurthy, Jain, Balasubramanya, & Vigneshwaran, 2011; Schwanninger, Rodrigues, Pereira, & Hinterstoisser, 2004; Sun, Sun, Zhao, & Sun, 2004). From these FTIR spectra, it was found that the acid hydrolysis reaction performed for obtaining the cellulose

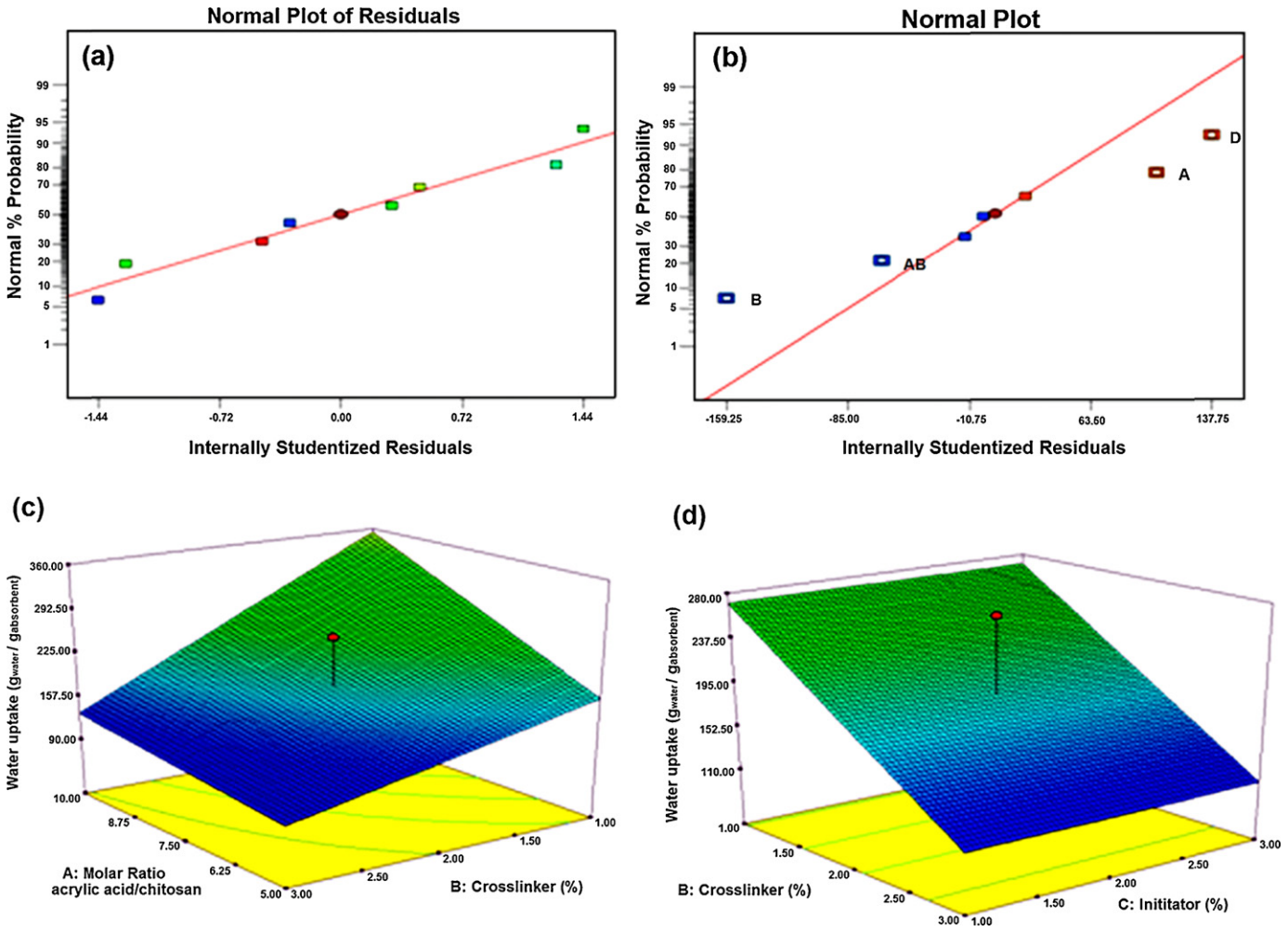

Fig. 1. (a) Normal plot of residuals, (b) normal plot and (c, d) response surfaces obtained from the 2^{4-1} fractional factorial design.

nanofibrils did not affect the chemical structure of the cellulosic fragments, but affect their morphologies.

The FTIR spectrum of chitosan-*graft*-poly(acrylic acid) exhibited a characteristic shoulder at 1686 cm^{-1} assigned to –COOH stretching and bands at 1573 and 1410 cm^{-1} assigned to asymmetric and symmetric stretching of C=O. The band at 1326 cm^{-1} should contribute to the stretching and bending vibrations of the C–N bond of the amide III band. The characteristic absorption bands of N–H (1598 and 1380 cm^{-1}) and C_3–OH (1094 cm^{-1}) of chitosan could not be found (Liu, Zheng, & Wang, 2010; Wang, Xie, Zhang, Zhang, & Wang, 2010); such information confirm that $-NH_2$, –NHCO, and –OH from chitosan took part in the grafting reaction with acrylic acid. Bands at 1457 (C–H), 1410, 1170, and 1070 cm^{-1} indicated the existence of poly(acrylic acid) chains (Chen & Tan, 2006; Zhang, Wang, & Wang, 2007; Zhang, Zhao, You, Qi, & Chen, 2007). The FTIR spectrum of chitosan-*graft*-poly(acrylic acid)/cellulose nanofibrils presented a similar pattern. Bands at 1169, 1118 and 1056 cm^{-1} are assigned to C–O–C asymmetric valence vibration, vibrational stretching C–C and C–O asymmetric pyran ring and C–O deformation in secondary alcohols and aliphatic ethers, regarding to cellulose nanofibrils, which confirms the hydrogel composite formation (Oh et al., 2005; Satyamurthy, Jain, Balasubramanya, & Vigneshwaran, 2011, Schwanninger et al., 2004; Sun et al., 2004).

The X-ray diffraction (XRD) pattern of cellulose nanofibrils showed that the cellulose nanocrystals present diffraction peaks at $2\theta = 14.5^\circ$, 16.3°, 22.4°, and 34.1° that are characteristic of 1 0 1, 1 0 1′, 0 0 2 and 0 4 0 plane positions typical of crystalline form from cellulose. The crystallinity index of cellulose nanofibrils (I_{cr}) was determined by the empirical method described by Segal, Creely, Martin, and Conrad (1959), according to equation:

$$I_{cr} = \left[\frac{I_{002} - I_{AM}}{I_{002}}\right] \times 100 \quad (3)$$

where I_{cr} is the crystalline index in percentage, I_{002} is the maximum intensity of diffraction corresponding to 0 0 2 plane of cellulose crystals (reflection attributed to crystalline areas, detected at angle $2\theta = 22.5^\circ$) and I_{AM} is the diffraction intensity reported at angle $2\theta = 18^\circ$ (reflection attributed to amorphous areas).

The hydrolysis reaction, performed to obtain the cellulose nanocrystals, increases the crystallinity index (I_{cr} 90.3%) of the fibers compared to cotton (I_{cr} 80%) due to the preference acidic attack in the amorphous regions in cellulose, which increases the level of the crystalline domains in obtained cellulose nanocrystals. The relative crystallinity index is about 90.3%, which is in agreement with other literature values (Elazzouzi-Hafraoui et al., 2008).

3.3. Morphologies of hydrogel composite

The changes on morphology of chitosan-*graft*-poly(acrylic acid) hydrogel promoted by addition of cellulose nanofibrils were investigated through SEM images (Fig. 2). As can be seen, chitosan-*graft*-poly(acrylic acid) hydrogel (Fig. 2a) shows interlaced network and highly porous morphology. The pores show small average size and are homogeneously distributed into the

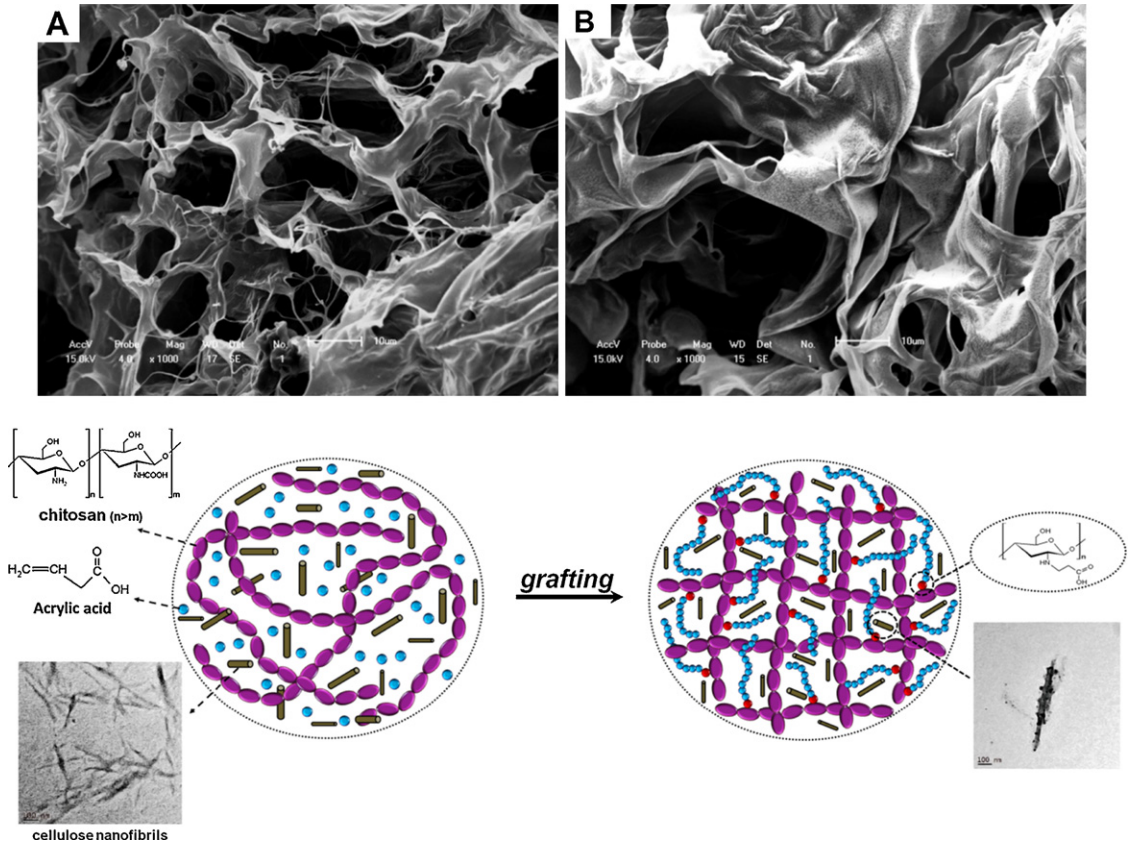

Fig. 2. SEM images of (a) chitosan-*graft*-poly(acrylic acid) and (b) chitosan-*graft*-poly(acrylic acid)/cellulose nanofibrils hydrogels composites (Mag 1000×, scale 10 μm) and scheme of chitosan-*graft*-poly(acrylic acid)/cellulose nanofibrils hydrogel composite formation.

hydrogel matrix, which could be associated with the lower liquid uptake capacity of chitosan-*graft*-poly(acrylic acid) hydrogel. The chitosan-*graft*-poly(acrylic acid)/cellulose nanofibrils hydrogel composite morphology (Fig. 2b) seems to be more irregular with large pores and foliaceous aspect. The presence of cellulose nanofibrils into the hydrogel matrix increases the amount of hydrophilic groups, which make diffusion of liquids inward the matrix easier and faster. This fact increases the average pore size as can be seen in the SEM image.

In view of the above-mentioned data, the formation mechanism of chitosan-*graft*-poly(acrylic acid)/cellulose nanofibrils hydrogel composite is sketched in Fig. 3. In addition, Fig. 3 shows TEM images of cellulose nanofibrils and dispersed into the chitosan-*graft*-poly(acrylic acid)/cellulose nanofibrils hydrogel matrix.

3.4. Effect of cellulose nanofibrils on swelling kinetics

Fig. 4 shows the swelling kinetics in aqueous media for the hydrogel composites (chitosan-*graft*-poly(acrylic acid)/cellulose nanofibrils) and for the blank sample cellulose nanofibrils (chitosan-*graft*-poly(acrylic acid)). The observed trends in the swelling kinetics are very similar. There were a quick increase in the degree of swelling during the first 30 min of immersion, reaching about 90% of the equilibrium value in this time range, followed by a slower process until the equilibrium was reached (W_{eq}) at around 60 min, values depending on the hydrogel. The introduction of cellulose nanofibrils within the chitosan-*graft*-poly(acrylic acid) network greatly improved the equilibrium of water absorbency capacity and decreased the necessary time to reach the equilibrium condition. The chitosan-*graft*-poly(acrylic acid) hydrogel presented water absorption capacity at equilibrium (W_{eq}) of 381 $g_{water}/g_{absorbent}$ while chitosan-*graft*-poly(acrylic acid)/cellulose nanofibrils hydrogel composite presented higher water absorption capability (W_{eq} = 486 $g_{water}/g_{absrobent}$, respectively).

Some of the characteristics collected from the swelling curves through the relations proposed according to Karadag, Uzum, and Saraydin (2005) are shown below:

$$\frac{t}{W} = A + Bt \tag{4}$$

where

$$A = \frac{1}{k_s W_t^2} \tag{5}$$

$$B = \frac{1}{W_t} \tag{6}$$

The A parameter corresponds to an initial swelling rate $[(dW/dt)_0]$ of the hydrogel, k_s is the constant rate for swelling, W_t is a theoretical swelling value at equilibrium and the initial swelling rate ($k_{is} = k_s W_{eq}^2$). W_t and k_s were calculated by fitting experimental

Table 3
Parameters obtained from swelling kinetics.

Hydrogel	W_{eq} [a]	W_t [b]	t_{eq} [c]	k_s [d]	k_{is} [e]
Chitosan-*graft*-poly(acrylic acid)	381 ± 10	389	46 ± 3	2.86×10^{-4}	41.52
Chitosan-*graft*-poly(acrylic acid)/cellulose nanofibrils	486 ± 12	488	35 ± 2	4.06×10^{-4}	95.90

[a] Equilibrium swelling ($g_{water}/g_{absorbent}$).
[b] Equilibrium theoretical swelling ($g_{water}/g_{absorbent}$).
[c] Equilibrium time (min).
[d] Rate of swelling [($g_{water}/g_{absorbent}$) min^{-1}].
[e] Initial swelling constant [($g_{water}/g_{absorbent}$) min^{-1}].

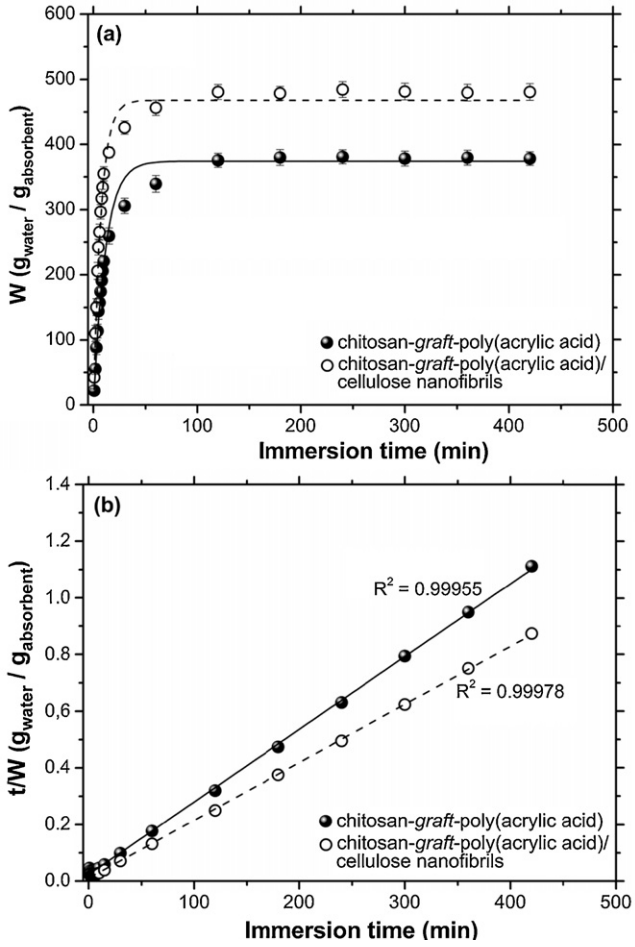

Fig. 3. (a) Swelling kinetic curves of chitosan-*graft*-poly(acrylic acid) (experiment 2) and chitosan-*graft*-poly(acrylic acid)/cellulose nanofibrils hydrogel composite with 10 wt% of cellulose nanofibrils (experiment 6) in distilled water and (b) *t*/*W versus t* graph for chitosan-*graft*-poly(acrylic acid) and chitosan-*graft*-poly(acrylic acid)/cellulose nanofibrils hydrogel composite with 10 wt% of cellulose nanofibrils.

data shown in Fig. 4a and b to Eqs. (4)–(6). The values associated to parameters of Eqs. (4)–(6) are presented in Table 3.

3.5. Swelling behavior at various pH and effect of salt solution on water absorbency

The swelling behavior of chitosan-*graft*-poly(acrylic acid) and chitosan-*graft*-poly(acrylic acid)/cellulose nanofibrils hydrogel composites at various pHs were observed with the use of buffer solutions at pHs 2–12, maintaining the ionic strength equal to 0.1. According to Fig. 4a, the absorbency of the optimized hydrogel increased as the pH increased from 2.0 to 8.0 and then decreased at pH higher than 8.0. Since the hydrogels show different swelling behaviors at various pHs, we investigated their pH-reversibility in the buffer solutions at pHs 2.0 and 8.0. Fig. 4b shows a step-wise reproducible swelling change of the hydrogel at 25 °C with alternating pH between 2.0 and 8.0. At pH 8.0, both the hydrogels (with and without filler) swell more due to anion–anion repulsive electrostatic forces, while, at pH 2.0, the hydrogels shrink within a few minutes due to protonation of carboxylate groups. This sharp swelling–deswelling behavior of the hydrogels makes them suitable candidates for controlled drug delivery systems. Such on–off switching behavior as reversible swelling and deswelling has been reported for other ionic hydrogels (Mahdavinia, Zohuriaan-Mehr, & Pourjavadi, 2004).

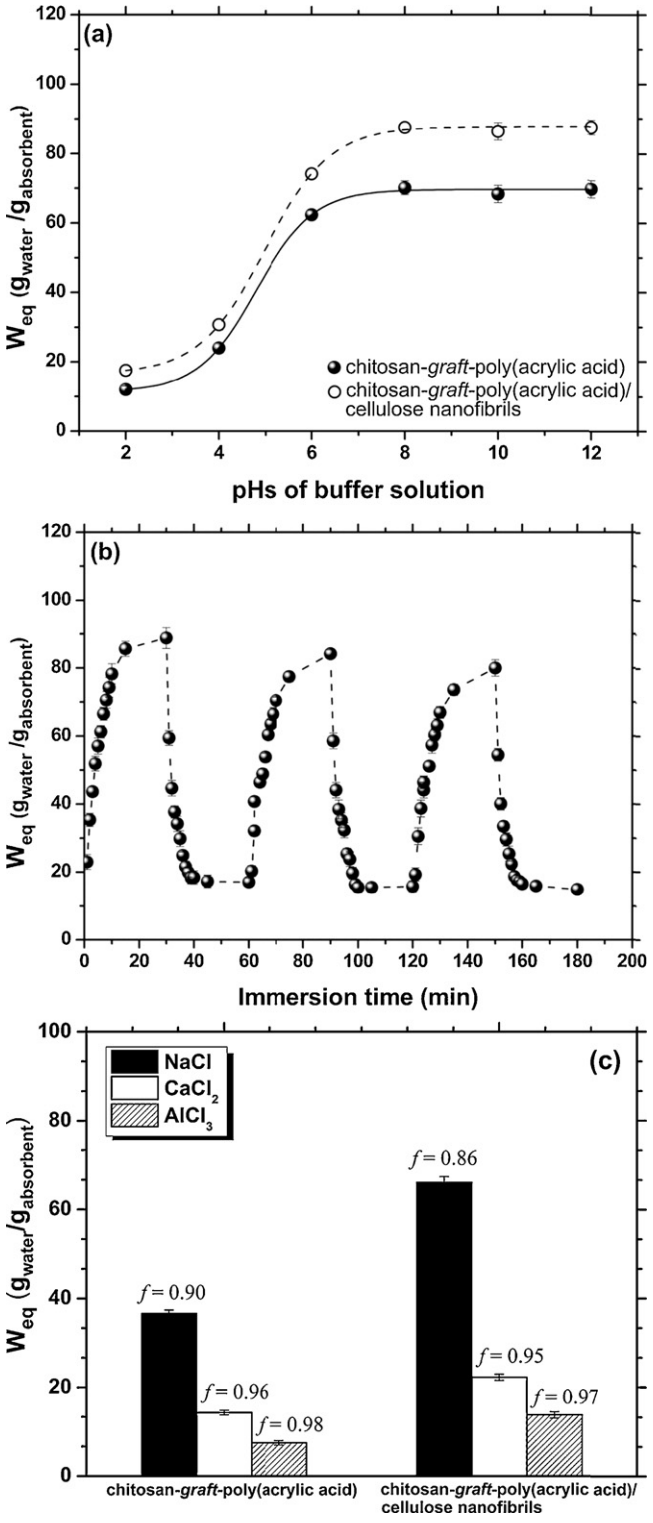

Fig. 4. (a) Effect of pH in the swelling properties of chitosan-*graft*-poly(acrylic acid) (experiment 2) and chitosan-*graft*-poly(acrylic acid)/cellulose nanofibrils hydrogel composite with 10 wt% of cellulose nanofibrils (experiment 6). (b) On–off switching behavior as reversible pulsatile swelling (pH 8.0) and deswelling (pH 2.0) of the chitosan-*graft*-poly(acrylic acid)/cellulose nanofibrils superabsorbent with 10 wt% of cellulose nanofibrils. The time interval between the pH changes was 30 min. (c) W_{eq} of chitosan-*graft*-poly(acrylic acid) and chitosan-*graft*-poly(acrylic acid)/cellulose nanofibrils hydrogel composites at aqueous solutions from different salts (conc. equal to 0.15 mg L^{-1}).

For both, chitosan-*graft*-poly(acrylic acid) and chitosan-*graft*-poly(acrylic acid)/cellulose nanofibrils, the variation in the swelling capacity can be attributed to changes in the protonation of the carboxylic groups from poly(acrylic acid) according to pH variations. When the hydrogels are swelled in the pH range of 2–4 the carboxylic groups from poly(acrylic acid), are in their neutral form (–COOH) and the hydrogel network did not undergo destabilization due to anion–anion repulsion. It should be noticed that the carboxylic groups from poly(acrylic acid) present pK_a close to 4.57. Therefore, the hydrogel matrix keeps itself entangled enough to prevent that a higher liquid content could be absorbed. When the pH of the media is increased to the range of 6–8, the carboxylic groups start to dissociate ($-COOH \rightarrow -COO^- + H^+$) and anion–anion repulsive forces destabilize the hydrogel matrix. This effect causes to the hydrogel matrix an expansion and the amount of liquid absorbed increases considerably as can be seen by the increase in the swelling curves (El-Hamshary, 2007). On the other hand, at higher pH conditions (pH > 8), most of $-COO^-$ groups change into –COOH groups due to excess of negatively charged groups in the media, which results in the decrease of repulsion among polymeric chains and consequentially leads to a decrease of liquid absorbency.

In this work, the influence of some ions (cations and anions) on swelling capability of hydrogels was tested by the addition of different saline solution, including monovalent (NaCl), divalent ($CaCl_2$) and trivalent ions, at 0.15 mol L^{-1} and at 25.0 °C, ($AlCl_3$) as the swelling fluid. To achieve a comparative measure of salt sensitivity of the hydrogels, a dimensionless salt sensitivity factor (f) is defined as follows:

$$f = 1 - \left(\frac{W_{saline}}{W_{water}}\right) \quad (7)$$

where W_{saline} and W_{water} are, respectively, the swelling capacity in saline solution and in deionized water. It is obvious that swelling decreasing is strongly depended on the "type" of salt added to the swelling medium. The effect of cation type (cations with different radius and charge) and sensitivity factor (f) on swelling behavior is shown in Fig. 4c. The higher cation charges the higher degree of crosslinking and the smaller swelling value. Therefore, the absorbency for the hydrogel in the studied salt solutions is in the order of monovalent > divalent > trivalent cations.

The f values (Fig. 4c) indicate that the chitosan-*graft*-poly(acrylic acid)/cellulose nanofibrils hydrogels undergo less influence to the presence of salt than the chitosan-*graft*-poly(acrylic acid). The increase in the ionic strength reduces the difference in the concentration of movable ions between the polymer matrix and the external solution (osmotic swelling pressure) and leads to an immediate contraction of gel. The decreasing is more significant to Ca^{2+} and Al^{3+} ions, which can be additionally caused by the complex formation ability of carboxamide or carboxylate groups including intramolecular and intermolecular complex formations, or because one multivalent ion is able to neutralize several charges inside the gel. Consequently, the crosslinking density of the network increases while water absorption capacity decreases.

4. Conclusion

Hydrogel composites based on chitosan-*graft*-poly(acrylic acid) and cellulose nanofibrils, which were obtained from cotton fibers, were successfully synthesized as confirmed by FTIR and XRD data. By the use of 2^{4-1} fractional factorial design, it was possible to evaluate that the crosslinker and filler amounts were the main effects controlling the water uptake. Besides, the addition of cellulose nanofibrils in the polymer matrix clearly improved the swelling capacity. In addition, SEM images showed that the hydrogel morphology changed due to the cellulose nanofibrils addition. The proposed statistical model presented high coefficient of determination ($R^2 = 0.988$). Furthermore, the swelling kinetics, the effect of pH and salt for the both compositions (with and without filler), which presented the best water uptake were evaluated. Both hydrogels, chitosan-*graft*-poly(acrylic acid) and chitosan-*graft*-poly(acrylic acid)/cellulose nanofibrils, showed responsive behavior in relation to pH and to the salt solution presenting good potential of application as devices for controlled release of solutes.

Acknowledgments

The authors would like to thank the financial support by FUNCAP (BPI 0280-106/08 and PIL – 139.01.00/09), CNPq (Proc. 507308/2010-7), and CAPES.

References

Azeredo, H. M. C., Mattoso, L. H. C., Avena-Bustillos, R. J., Filho, G. C., Munford, M. L., Wood, D., et al. (2010). Nanocellulose reinforced chitosan composite films as affected by nanofiller loading and plasticizer content. *Journal of Food Science*, *75*, N1–N7.

Bajpai, A. K. & Giri, A. (2002). Swelling dynamics of a macromolecular hydrophilic network and evaluation of its potential for controlled release of agrochemicals. *Reactive & Functional Polymers*, *53*, 125–141.

Chen, Y. & Tan, H. M. (2006). Crosslinked carboxymethylchitosan-*graft*-poly(acrylic acid). Copolymer as a novel superabsorbent polymer. *Carbohydrate Research*, *341*, 887–896.

De Mesquita, J. P., Donnici, C. L. & Pereira, F. V. (2010). Biobased nanocomposites from layer-by-layer assembly of cellulose nanowhiskers with chitosan. *Biomacromolecules*, *11*, 473–480.

Ebringerová, A., Hromádková, Z. & Heinze, T. (2005). Hemicellulose. *Advances in Polymer Science*, *186*, 1–67.

Elazzouzi-Hafraoui, S., Nishiyama, Y., Putaux, J. L., Heux, L., Dubreuil, F. & Rochas, C. (2008). The shape and size distribution of crystalline nanoparticles prepared by acid hydrolysis of native cellulose. *Biomacromolecules*, *9*, 57–65.

El-Hamshary, H. (2007). Swelling and diffusion behaviors of pH sensitive poly (acrylamide-co-itaconic acid) hydrogels. *European Polymer Journal*, *43*, 4830–4839.

Fajardo, A. R., Piai, J. F., Rubira, A. F. & Muniz, E. C. (2010). Time- and pH-dependent self-rearrangement of a swollen polymer network based on polyelectrolytes complexes of chitosan/chondroitin sulfate. *Carbohydrate Polymers*, *80*, 934–941.

Hill, R. J. (2007). Electric-field-enhanced transport in polyacrylamide hydrogel nanocomposites. *Journal of Colloid Interface Science*, *316*, 635–644.

Karadag, E., Uzum, O. B. & Saraydin, D. (2005). Water uptake in chemically crosslinked poly(acrylamide-co-crotonic acid) hydrogels. *Materials Design*, *26*, 265–274.

Li, A., Liu, R. & Wang, A. (2005). Preparation of starch-graft-poly(acrylamide)/attapulgite superabsorbent composite. *Journal of Applied Polymer Science*, *98*, 1351–1357.

Li, Q., Zhou, J. & Zhang, L. (2009). Structure and properties of the nanocomposite films of chitosan reinforced with cellulose whiskers. *Journal of Polymer Science. Part B: Polymer Physics*, *47*, 1069–1077.

Liang, S., Zhang, L. N., Li, Y. N. & Xu, J. (2007). Fabrication and properties of cellulose hydrated membrane with unique structure. *Macromolecular Chemistry and Physics*, *208*, 594–602.

Liu, Y., Zheng, Y. & Wang, A. (2010). Enhanced adsorption of methylene blue from aqueous solution by chitosan-g-poly (acrylic acid)/vermiculite hydrogel composites. *Journal of Environmental Sciences*, *22*, 486–493.

Mahdavinia, G. R., Zohuriaan-Mehr, M. J. & Pourjavadi, A. (2004). Modified chitosan III, superabsorbency, salt- and pH-sensitivity of smart ampholytic hydrogels from chitosan-g-PAN. *Polymer for Advanced Technology*, *15*, 173–181.

Muzzarelli, R. A. A. (2009). Chitins and chitosans for the repair of wounded skin, nerve, cartilage and bone. *Carbohydrate Polymers*, *76*, 167–182.

Muzzarelli, R. A. A. (2011). New techniques for optimization of surface area and porosity in nanochitins and nanochitosans. In R. Jayakumar, A. Prabaharan, & R. A. A. Muzzarelli (Eds.), *Advances in polymer science: Chitosan for biomaterials* (pp. 167–186). Berlin: Springer-Verlag.

Nakagaito, A. N., Fujimura, A., Sakai, T., Hama, Y. & Yano, H. (2009). Production of microfibrillated cellulose (MFC)-reinforced polylactic acid (PLA) nanocomposites from sheets obtained by a papermaking-like process. *Composites Science and Technology*, *69*, 1293–1297.

Oh, S. Y., Yoo, D. I., Shin, Y. & Seo, G. (2005). FTIR analysis of cellulose treated with sodium hydroxide and carbon dioxide. *Carbohydrate Research*, *340*, 417–428.

Omidian, H., Rocca, J. G. & Park, K. (2005). Advances in superporous hydrogel. *Journal of Controlled Releases*, *102*, 3–12.

Paulino, A. T., Guilherme, M. R., Almeida, E. A. M. S., Pereira, A. G. B., Muniz, E. C. & Tambourgi, E. B. (2009). One-pot synthesis of a chitosan-based hydrogel as a potential device for magnetic biomaterial. *Journal of Magnetic Materials*, *321*, 2636–2645.

Peresin, M. S., Habibi, Y., Vesterinen, A.-H., Rojas, O. J., Pawlak, J. J. & Seppälä, J. V. (2010). Effect of moisture on electrospun nanofiber composites of poly(vinyl alcohol) and cellulose nanocrystals. *Biomacromolecules*, *11*, 2471–3247.

Satyamurthy, P., Jain, P., Balasubramanya, R. H. & Vigneshwaran, N. (2011). Preparation and characterization of cellulose nanowhiskers from cotton fibres by controlled microbial hydrolysis. *Carbohydrate Polymers*, *83*, 122–129.

Schwanninger, M., Rodrigues, J. C., Pereira, H. & Hinterstoisser, B. (2004). Effects of short-time vibratory ball milling on the shape of FT-IR spectra of wood and cellulose. *Vibrational Spectroscopy*, *36*, 23–40.

Segal, L., Creely, J. J., Martin, A. E. & Conrad, C. M. (1959). An empirical method for estimating the degree of crystallinity of native cellulose using the X-ray diffractometer. *Textile Research Journal*, *29*, 786–794.

Sun, J. X., Sun, X. F., Zhao, H. & Sun, R. C. (2004). Isolation and characterization of cellulose from sugarcane bagasses. *Polymer Degradation and Stability*, *84*, 331–339.

Teixeira, E. M., Pasquini, D., Curvelo, A. A. S., Corradini, E., Belgacem, M. N. & Dufresne, A. (2009). Cassava bagasse cellulose nanofibrils reinforced thermoplastic cassava starch. *Carbohydrate Polymers*, *78*, 422–431.

Wang, H., Li, W., Luz, Y. & Wang, Z. (1997). Studies on chitosan and poly(acrylic acid) interpolymer complex. I. Preparation, structure, pH-sensitivity, and salt sensitivity of complex-forming poly(acrylic acid): Chitosan semi-interpenetrating polymer network. *Journal of Applied Polymer Science*, *65*, 1445–1453.

Wang, Q., Xie, X., Zhang, X., Zhang, J. & Wang, A. (2010). Preparation and swelling properties of pH-sensitive composite hydrogel beads based on chitosan-g-poly (acrylic acid)/vermiculite and sodium alginate for diclofenac controlled release. *International Journal of Biological Macromolecules*, *46*, 356–362.

Zhang, J. P., Wang, Q. & Wang, A. Q. (2007). Synthesis and characterization of chitosan-*graft*-poly(acrylic acid)/attalpulgite superabsorbent composites. *Carbohydrate Polymers*, *68*, 367–374.

Zhang, J., Zhao, S., You, C., Qi, H. & Chen, C. (2007). Rapid hydration preparation of calcium based sorbent made from lime and fly ash. *Industrial and Engineering Chemical Research*, *46*, 5340–5345.

Zhang, L., Rakotondradany, F., Myles, A. J., Fenniri, H. & Webste, T. J. (2009). Arginine–glycine–aspartic acid modified rosette nanotube-hydrogel composites for bone tissue engineering. *Biomaterials*, *30*, 1309–1320.

Zheng, Y., Liu, Y. & Wang, A. (2011). Fast removal of ammonium ion using a hydrogel optimized with response surface methodology. *Chemical Engineering Journal*, *171*, 1201–1208.

Zhou, C., Wu, Q., Yue, Y. & Zhang, Q. (2011). Application of rod-shaped cellulose nanocrystals in polyacrylamide hydrogels. *Journal of Colloid and Interface Science*, *353*, 116–123.